Proceedings of the 9th U.S. National and 10th Canadian Conference on Earthquake Engineering
Compte Rendu de la 9ième Conférence Nationale Américaine et
10ième Conférence Canadienne de Génie Parasismique
July 25-29, 2010, Toronto, Ontario, Canada • Paper No 544

# USE OF SMA AND BUCKLING RESTRAINED BRACES TO REDUCE SEISMIC RESIDUAL DEFORMATIONS IN LOW-RISE RC FRAMES

**M.A. Youssef[1], M.E. Mashaly[2], and H. Abou-Elfath[3]**

## ABSTRACT

Concentric bracing systems have proven to be effective in limiting the lateral drifts of Reinforced Concrete (RC) frames. One of the known deficiencies for these systems is the expected residual deformations following a seismic event. This paper focuses on evaluating the effect of using Buckling Restrained Braces (BRBs) and Shape Memory Alloy Braces (SMABs) on the seismic performance of a three-storey RC building. Two RC frames are designed utilizing both BRBs and SMABs and analyzed using pushover and dynamic analyses. The SMAB system is found to significantly reduce seismic residual deformations. However, this advantage is lost at peak ground accelerations close to the peak ground acceleration causing failure of the frame.

## Introduction

Moment-resisting frames experience large lateral drifts during seismic events. These drifts lead to extensive damage in non-structural elements. Concentrically braced frames provide a solution to this problem by limiting seismic lateral drifts. Their inelastic deformations occur due to brace yielding in tension and brace buckling in compression. Disadvantages of concentrically braced frames include: (1) poor energy dissipation due to buckling of the compression braces, and (2) seismic residual deformations. This paper explores methods to overcome these disadvantages.

Restraining the buckling of bracing members can be achieved by utilizing BRBs. It consists of a steel core that is susceptible to inelastic deformations during earthquake ground motions and a casing (sleeve) for restraining buckling of the core element (Sabelli et al. 2003). The axial stresses are resisted by the steel core only. Since the brace is not allowed to buckle, it develops a uniform axial strain.

Superelastic Shape Memory Alloys (SMAs) are smart alloys that are able to return to their original shape upon removal of loading. Dolce et al. (2004) found that SMABs can provide a good re-centring capability when applied to a two-storey single-bay concrete frame. Auricchio et al. (2006) compared the seismic performance of steel braces and superelastic SMABs when implemented in three- and six-storey buildings. They found that buildings with SMABs had reduced inter-storey and residual drifts.

[1] Associate Professor, The University of Western Ontario, Dept. of Civil & Env. Eng., London, ON N6A 5B9.
[2] Ph.D. Candidate, The University of Western Ontario, Dept. of Civil & Env. Eng., London, ON N6A 5B9
[3] Assistant Professor, Department of structural Engineering, Alexandria University, Alexandria, Egypt

The objective of this paper is to evaluate the potential of using BRBs and SMABs to control seismic damage of low-rise RC frames. The following sections provide details about the design, analysis, and results of two concrete frames that utilize both bracing systems.

## Frame Design

A three-storey concrete office building is considered for this study. The building floor plan and elevation are shown in Figs. 1a and 1b, respectively. The storey height is 3.6 m. The two exterior frames are assumed to be braced using a stacked chevron (inverted-V) pattern. The building is designed according to the American standard (ACI 2008) and the international building code (IBC 2006). The building is assumed to be located in Berkley, California with site class (C). The design spectral accelerations at short period ($S_{DS}$) and at one second ($S_{D1}$) are 1.10g and 0.59g, respectively. A response modification factor (R), an over-strength factor ($\Omega_o$), and deflection amplification factor ($C_d$) of 8, 2.5, and 5, respectively, are used. The slab thickness is taken equal to 180 mm. The superimposed dead loads are assumed to be 2.4 kN/$m^2$. The design base shear is found to be 507 kN. Details of the beams and columns of the BRB Frame (BRBF) and SMAB Frame (SMABF) are shown in Fig. (2).

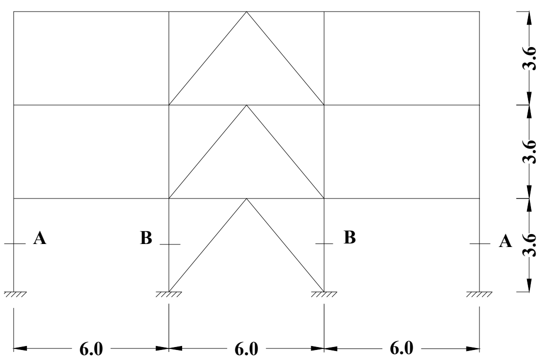


Figure 1a: Building Elevation
(all dimensions are in meters)

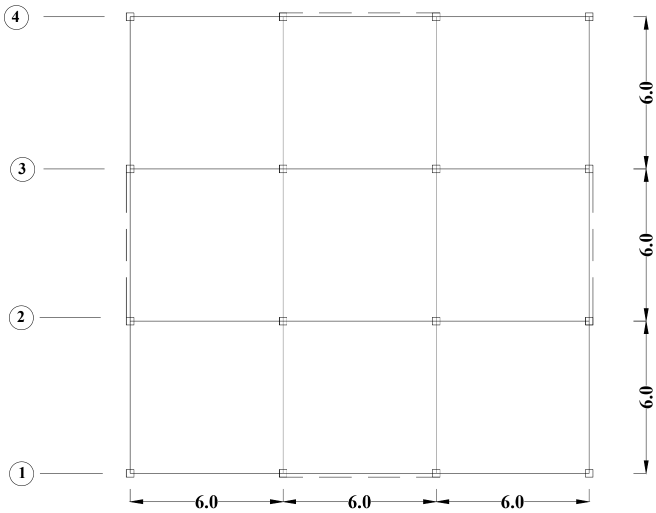


Figure 1b: Building Plan
(All dimensions are in meters)

The core of a BRB is divided into three zones; the yielding zone (a reduced section restrained by the casing), transition zones (on both sides of the yielding zone) of larger cross-sectional area, and connection zones that are connected to the frame by gusset plates as shown in Fig. (3) (Sabelli et al. 2003). The stiffness of a BRB is calculated assuming a yield length equal to 50% of the brace length as the yielding segment is the only source for the brace flexibility. The beam connected to the bracing members is designed to resist modest seismic loads because of the balance between the brace capacity in compression and tension.

The only difference between the SMABF and the BRBF is that the BRBs are replaced with superelastic SMABs. These braces consist of rigid elements connected to the frame using SMA bars. Similar braces were used by Auricchio et al. (2006). The SMABs are designed to provide the same initial axial stiffness and yield force as the BRBs. The cross sectional areas of the SMABs are 642 mm$^2$, 539 mm$^2$, and 326 mm$^2$ for the 1$^{st}$, 2$^{nd}$, and 3$^{rd}$ storey, respectively. The length of the SMA bars is 650 mm for all floors.

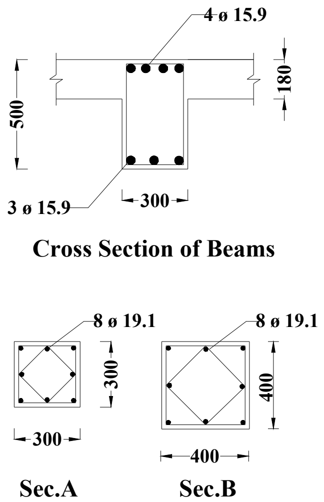


Figure 2: Details of beams and columns (all dimensions are in millimetres)

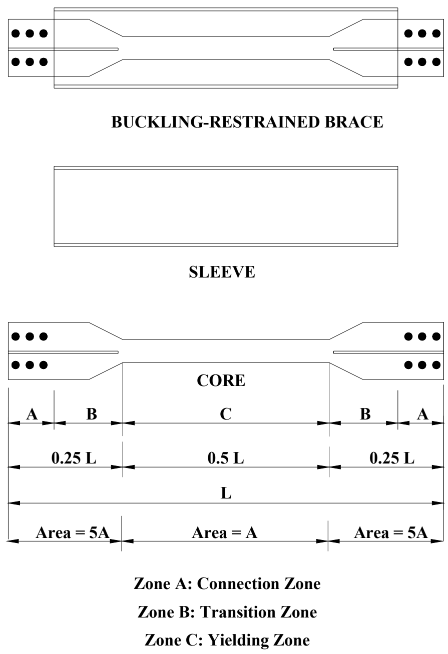


Figure 3: Detail of a buckling restrained brace

## Computer Modelling

Static and nonlinear time historey analyses are carried out using the SeismoStruct computer program (SeismoSoft 2007). Beams and columns are modelled using a uniaxial nonlinear constant confinement concrete model that follows the constitutive relationship proposed by Mander et al. (1988) and the cyclic rules proposed by Martinez-Rueda and Elnashai (1997). Beams and columns are assumed to be split into four elements to capture accurately the spread of inelasticity over the element length. Models for both superelastic SMABs and BRBs are shown in Fig. (4) (Auricchio et al. 2006). Material properties of the steel and SMA are summarised in table (1).

Table 1: Material properties

| | |
|---|---|
| Initial modulus of elasticity of steel | 200,000 MPa |
| Initial modulus of elasticity of SMA | 68,200 MPa |
| Yield strength of steel brace | 360 MPa |
| Yield strength of reinforcing steel bars | 413 MPa |
| Austenite to martensite starting stress ($\sigma_S^{AS}$) | 480 MPa |
| Austenite to martensite finishing stress ($\sigma_F^{AS}$) | 540 MPa |
| Martensite to austenite starting stress ($\sigma_S^{SA}$) | 260 MPa |
| Martensite to austenite finishing stress ($\sigma_F^{SA}$) | 120 MPa |
| Maximum recoverable strain ($\varepsilon_L$) | 6.2 % |

The BRB is modelled as a pin-ended member using a uniaxial bilinear stress-strain model with kinematic strain hardening. The SMAB is modelled based on a uniaxial model proposed by (Auricchio and Sacco 1997). The model assumes a constant stiffness for both the fully austentic and fully martensitic behaviour.

## Pushover Analysis

Static pushover analyses are conducted for the BRBF and the SMABF using the lateral load distribution presented in the code. The response parameters considered in the evaluation of the braced frames are; the roof drift ratio, the storey drift ratio, and the Maximum Storey Drift Ratio (MSDR).The crushing strain of the unconfined concrete, $\zeta_{u(unconfined)}$, is assumed 0.0035. The crushing strain for the confined concrete, $\zeta_{u\ (confined)}$, is found to be varying from 0.015 to 0.05 (Paulay and Priestley 1992). The value of the crushing strain is evaluated in this paper using the following equation:

$$\zeta_{u\ (confined)} = \zeta_{u\ (unconfined)} + \frac{1.4\rho_s f_y \zeta_{sm}}{K_h f_{c'}} \quad \text{(Park and Paulay 1972)} \qquad (1)$$

where $\rho_s$ is the ratio of the volume of transverse reinforcement of concrete core measured to the outside of the transverse reinforcement, $\zeta_{sm}$ is the steel strain at maximum tensile stress, $k_h$ is the confinement factor, and $f_y$ is the yield strength of steel reinforcement. Failure of the concrete frame is assumed to occur when the core concrete at both ends of two or more columns located in the same storey reaches the crushing state.

The capacity curves of the BRBF and SMABF are shown in Fig. (5). The base shears at failure are 2.58 and 5.38 times the design base shear, respectively. The two frames yielded at the same roof drift ratio (0.23%) as was assumed in the design stage. The SMABF failed at a lower roof drift. The distributions of the storey drift ratios of both frames at failure are shown in Fig. (6a). The figure shows that the maximum drifts were at the second floor and that their values at failure for the SMABF and BRBF are 13.85% and 18.56%, respectively. The distributions of the storey drift ratios of both frames at failure of the SMABF are shown in Fig. (6b). The sequence of yielding in brace members and core concrete crushing in beams and columns of the BRBF and the SMABF are shown in Fig. (7).

Yielding of brace members of the BRBF started at a roof drift ratio of 0.23%. At a ratio of 0.44%, all brace members had yielded. The first core concrete crushing was observed in a first storey beam (location 5 in Fig. 7a) at a roof drift ratio of 1.77%. Increasing the drift to 3.39% resulted in a number of concrete crushed sections (locations 6 to 11 in Fig. 7a). At a drift of 15.54%, two of the first floor columns reached crushing at both of their ends (locations 12 and 33 in Fig. 7a).

Yielding of brace members of the SMABF started at a roof drift ratio of 0.23%. At a ratio of 0.44%, all brace members had yielded. The first core concrete crushing was observed at a roof drift ratio of 2.45% in a first storey beam (location 5 in Fig. 7b). Increasing the drift to 3.80% resulted in a number of concrete crushed sections (locations 5 to 13 in Fig. 7b). At a drift of 8.93%, two of the first floor columns reached crushing at both of their ends (locations 14 and 30 in Fig. 7b).

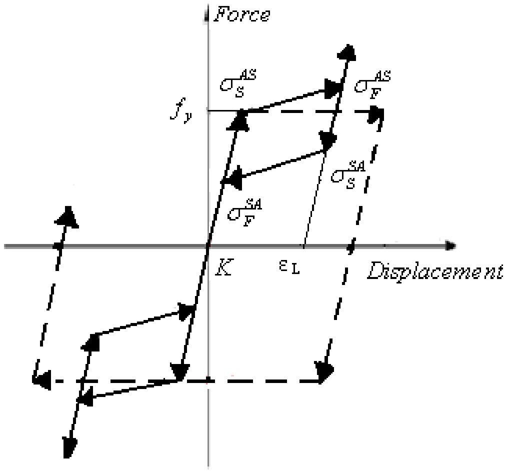


Figure 4: Models for BRBs (dashed line) and superelastic SMABs (continuous line).

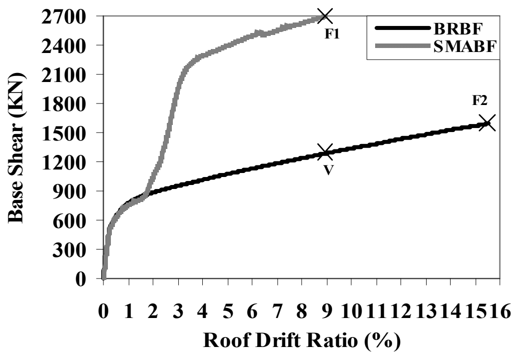


Figure 5: Pushover capacity curves

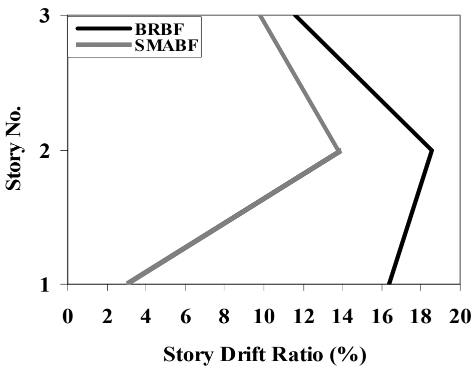


Figure 6a: The distributions of the storey drift ratios at failure (points F1 and F2 in Fig. 5)

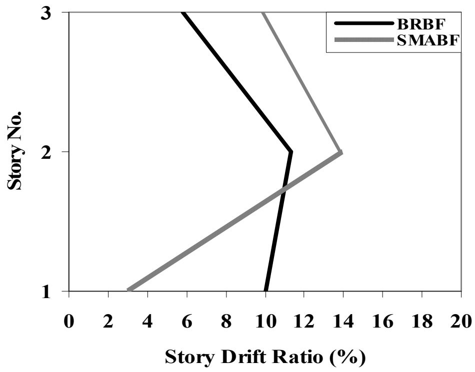


Figure 6b: The distributions of the storey drift ratios at failure of the SMABF (points F1 and V in Fig. 5)

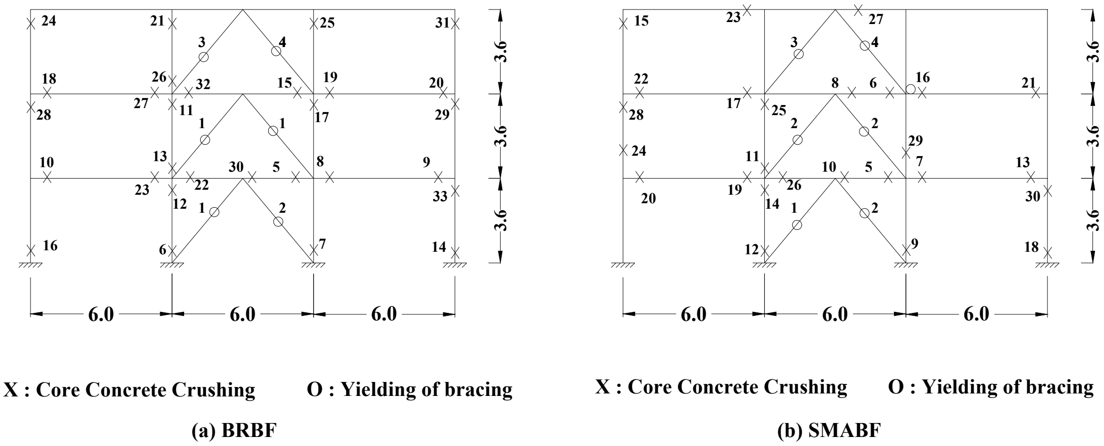


Figure 7: Sequence of brace yielding and core concrete crushing

**Dynamic Analysis**

The structural mass is assumed to be lumped at the beam column joints. Dynamic analyses of the frames are performed using a time step increment of 0.005 second. The effect of the geometric non-linearity (P-Δ effect) is considered in the analysis. Vamvatsikos and Cornell (2004) recommended the use of 20 records from three earthquakes (1979 Imperial Valley; 1987 Superstition Hills; and 1989 Loma Prieta) to analyze low- and mid-rise buildings. The characteristics of these 20 records are summarized in table (2). These records are selected to cover a wide range of frequency contents and durations and are utilized in the present study. The dynamic analyses of the frames are carried out using scaled versions of the selected twenty records. Scale factors are selected to achieve peak ground accelerations PGA of 0.5g, 0.75g, 1.0g, and 1.25g. The response parameters considered in the evaluation of the frames are; the roof drift ratio, the residual roof drift ratio, the storey drift ratio, and the maximum storey drift ratio.

Table 2: Selected Earthquake Ground Motion Records

| Record No. | Event | Year | Record Station | $\Phi^1$ | $M^{*2}$ | $R^{*3}$(Km) | PGA(g) |
|---|---|---|---|---|---|---|---|
| 1 | Imperial Valley | 1979 | Cucapah | 85 | 6.9 | 23.6 | 0.309 |
| 2 | Imperial Valley | 1979 | Chihuahua | 282 | 6.5 | 28.7 | 0.254 |
| 3 | Imperial Valley | 1979 | El Centro Array # 13 | 140 | 6.5 | 21.9 | 0.117 |
| 4 | Imperial Valley | 1979 | El Centro Array # 13 | 230 | 6.5 | 21.9 | 0.139 |
| 5 | Imperial Valley | 1979 | Plaster City | 45 | 6.5 | 31.7 | 0.042 |
| 6 | Imperial Valley | 1979 | Plaster City | 135 | 6.5 | 31.7 | 0.057 |
| 7 | Imperial Valley | 1979 | Westmoreland Fire Sta. | 90 | 6.5 | 15.1 | 0.074 |
| 8 | Imperial Valley | 1979 | Westmoreland Fire Sta. | 180 | 6.5 | 15.1 | 0.11 |
| 9 | Loma Prieta | 1989 | Agnews State Hospital | 90 | 6.9 | 28.2 | 0.159 |
| 10 | Loma Prieta | 1989 | Anderson Dam | 270 | 6.9 | 21.4 | 0.244 |
| 11 | Loma Prieta | 1989 | Coyote Lake Dam | 285 | 6.5 | 22.3 | 0.179 |
| 12 | Loma Prieta | 1989 | Hollister Diff. Array | 255 | 6.9 | 25.8 | 0.279 |
| 13 | Loma Prieta | 1989 | Hollister Diff. Array | 165 | 6.9 | 25.8 | 0.269 |
| 14 | Loma Prieta | 1989 | Holister South & Pine | 0 | 6.9 | 28.8 | 0.371 |
| 15 | Loma Prieta | 1989 | Sunnyvale Colton Ave | 270 | 6.9 | 28.8 | 0.207 |
| 16 | Loma Prieta | 1989 | Sunnyvale Colton Ave | 360 | 6.9 | 28.8 | 0.209 |
| 17 | Superstition Hill | 1987 | Wildlife Liquefaction Array | 90 | 6.7 | 24.4 | 0.18 |
| 18 | Superstition Hill | 1987 | Wildlife Liquefaction Array | 360 | 6.7 | 24.4 | 0.2 |
| 19 | Loma Prieta | 1989 | WAHO | 0 | 6.9 | 16.9 | 0.37 |
| 20 | Loma Prieta | 1989 | WAHO | 90 | 6.9 | 16.9 | 0.638 |

[1] Component, [2] Moment Magnitude, [3] Closest Distance to Fault Rupture

## Roof Drift Response

Fig. (8a) shows the variation of the mean and the (mean+2 x standard deviation) of the Maximum Roof Drift Ratio (MRDR) of both frames with the PGA value. The BRBF had an average MRDR of 0.75%, 1.36%, 2.07%, and 3.41% at PGA values of 0.5g, 0.75g, 1.0g, and 1.25g, respectively, whereas the SMABF had an average MRDR of 1.11%, 1.72%, 2.30%, and 3.00% at the same PGA values. The SMABF experienced higher roof drift ratio at lower PGA values (PGA≤1.0g). This is due to the lower stiffness of SMAB relative to the BRB. At intensities of peak ground accelerations much higher than the design ground acceleration (at PGA=1.25g), the BRBF had higher drifts.

## Residual Roof Drift Response

Fig. (8b) shows the variation of the mean and the (mean+2 x standard deviation) of the Residual Roof Drift Ratio (RRDR) of both frames with the PGA value. The BRBF had an average RRDR of 0.09%, 0.24%, 0.29%, and 0.30% at PGA values of 0.5g, 0.75g, 1.0g, and 1.25g, respectively. The SMABF had an average RRDR of 0.02%, 0.04%, 0.12%, and 0.21% at the same PGA values.

At PGA close to the design value, seismic loads are resisted by the bracing members. The RRDR of the SMABF at PGA values close to the design value is much lower than that of the BRBF because of the re-centring capability of the SMA material, maximum difference of about 83%. At PGA of 1.25 (much higher than the design acceleration), brace members reached their yield strength and thus seismic loads are resisted by both the bracing members and the concrete frame. The inelasticity experienced by the concrete frame led to a significant reduction in the difference between the RRDR of both frames.

## Storey Drift Response

Fig. (8c) shows the variation of the mean and the (mean+2 x standard deviation) of the MSDR of both frames with the PGA value. The BRBF had an average MSDR of 1.08%, 2.02%, 3.08%, and 4.54% at PGA values of 0.5g, 0.75g, 1.0g, and 1.25g, respectively. The SMABF had an average MSDR of 1.52%, 2.40%, 3.13%, and 4.12% at the same PGA values. The SMABF experienced higher storey drift ratio at lower PGA values (PGA≤1.0g). At intensities of peak ground accelerations much higher than the design ground acceleration (at PGA=1.25g), the BRBF had higher drifts.

The distributions of the mean values of storey drift ratios of both frames at different PGA values are shown in Fig. (9). The figure shows that the storey drift ratios of SMABF are almost uniform at all PGA values and those of the BRBF are almost uniform at PGA ≤ 0.5 g.

## Failure Mechanism

The sequence of brace yielding and core concrete crushing of both frames at different PGA values are shown in figures 10a, 10b, 11a, 11b, 12a, 12b, 13a, and 13b. These results are based on scaled versions of the Loma Prieta earthquake (record no. 13). For both frames, yielding occurred in all brace members for all of the considered PGA values. In case of BRBF, a PGA value of 0.75g caused core concrete crushing in one of the beams and in two base columns at one of their ends. For the SMABF and for the same PGA, core concrete crushing was observed in four of the beams and was not observed in any of the columns.

At a PGA value of 1.0g, the BRBF experienced core concrete crushing at six locations of the first storey beams and at one of the ends of three of the first floor columns. For the SMABF and for the same PGA, core concrete crushing was observed at one of the ends of two of the first storey columns and at 15 beam locations.

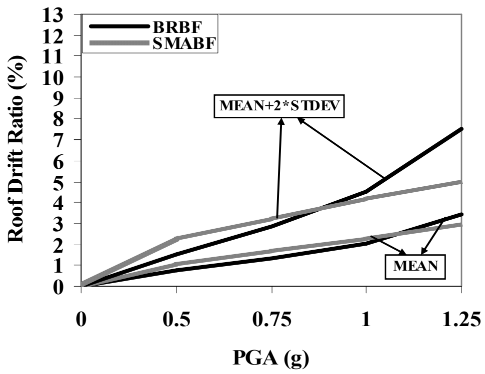


Figure 8a: Variation of the mean and (mean + 2 x standard deviation) of the MRDR with the PGA value

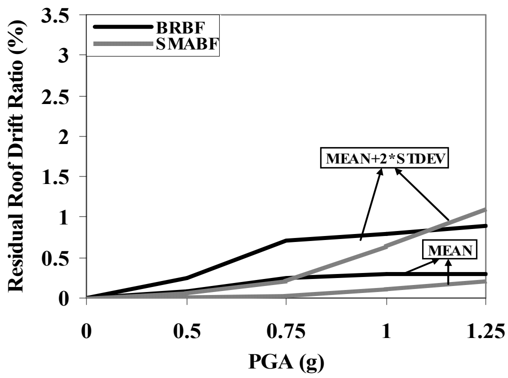


Figure 8b: Variation of the mean and (mean + 2 x standard deviation) of the RRDR with the PGA value

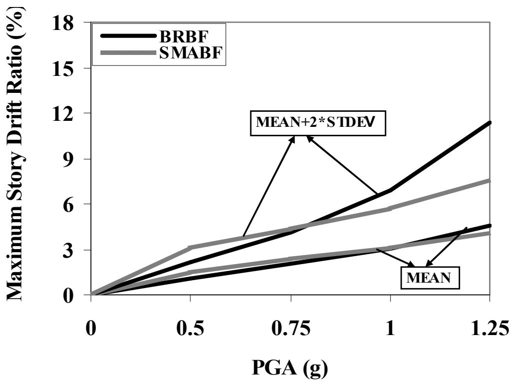


Figure 8c: Variation of the mean and (mean + 2 x standard deviation) of the MSDR with the PGA value

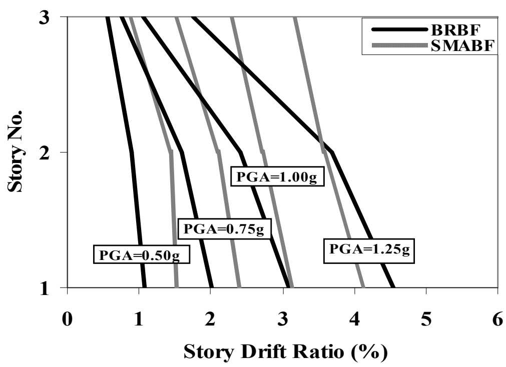


Figure 9: The distributions of the mean values of the storey drift ratios at different PGA values

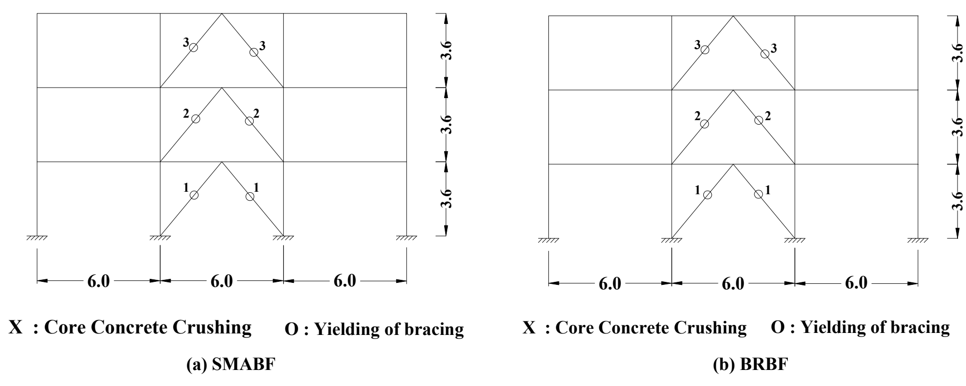


Figure 10: The sequence of brace yielding and core concrete crushing at PGA= 0.50g

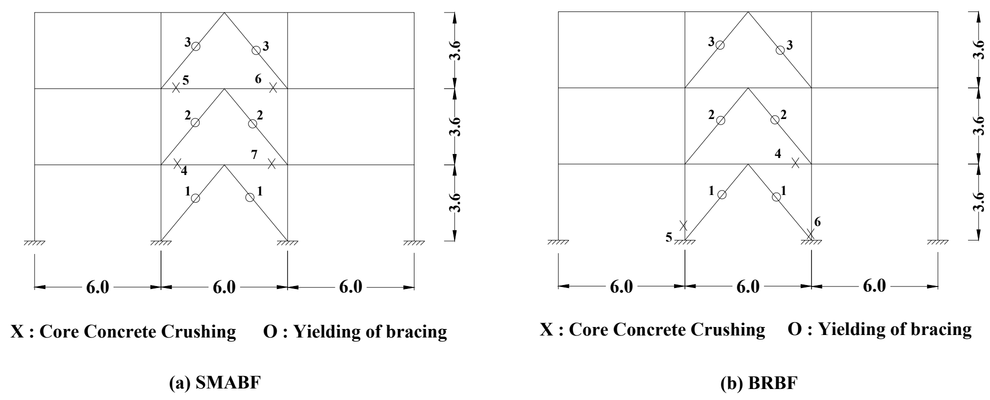


Figure 11: The sequence of brace yielding and core concrete crushing at PGA= 0.75g

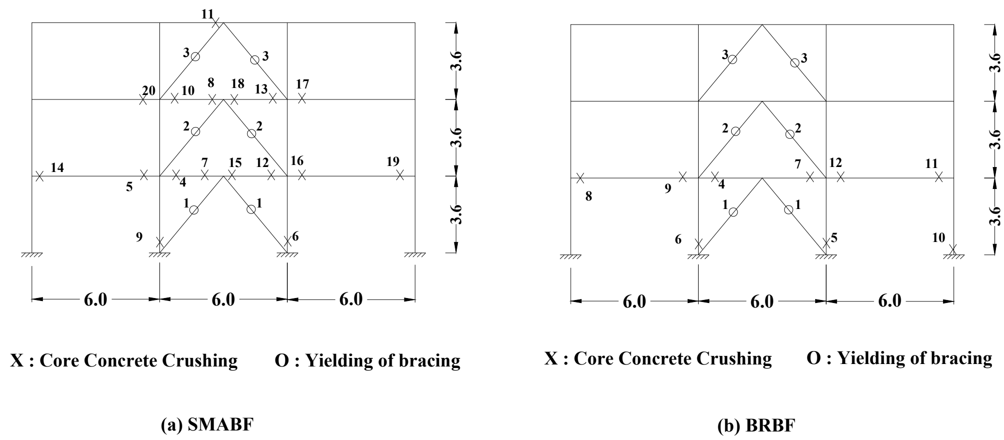


Figure 12: The sequence of brace yielding and core concrete crushing at PGA= 1.00g

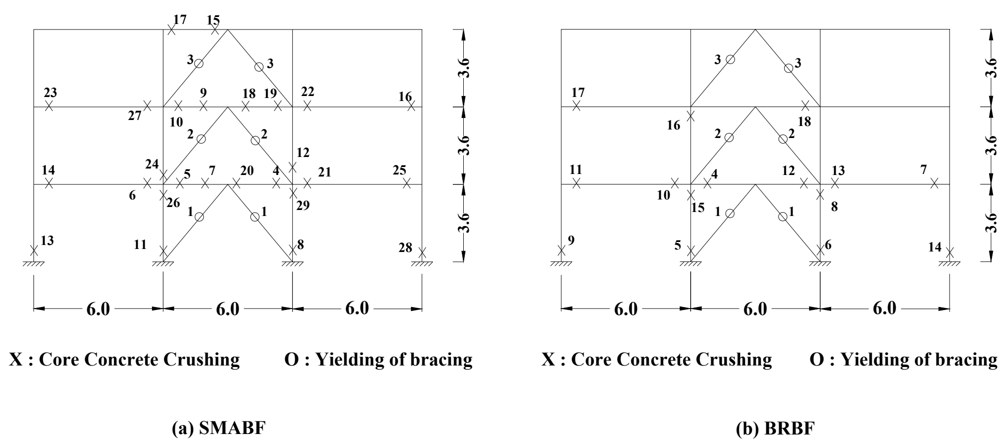


Figure 13: The sequence of brace yielding and core concrete crushing at PGA= 1.25g

At PGA of 1.25g, the BRBF had core concrete crushing at 7 column locations and 8 beam locations. The SMABF experienced crushing at 8 column locations and 18 beam locations. For both frames, two of the first storey columns crushed at both of their ends defining collapse of the frame. The previous results indicates that at lower values of PGA (at PGA=0.50g, 0.75g), the SMABF underwent less damage and experienced better response than the BRBF. At higher PGA values (at PGA=1.0g, 1.25g), performance of both frames was similar.

## Summary and Conclusions

This paper evaluates the use of superelastic SMABs and BRBs in low-rise RC frames. A three-storey office building is designed utilizing both bracing systems. Static and nonlinear time historey analyses are evaluated for both the SMABF and BRBF. The results of the static analysis show that at early stages of static pushover loading, the SMABF exhibited better response than the BRBF. At higher deformations, the response of the BRBF was better.

Results of the dynamic analysis led to the following conclusions:

(1) At PGA values close to the design PGA, use of superelastic SMA bars as bracing system in RC frames lead to significant reduction in seismic residual deformations. The reduction of the residual roof drift reached 83% when the behaviour of the SMABF and BRBF was compared.

(2) At PGA values that are close to the failure PGA, the difference between the residual deformations of the SMABF and the BRBF was minor. This is attributed to the fact that residual deformations at this stage are mainly resulting from inelasticity of the concrete frame itself.

## References

Auricchio F. and Sacco E. (1997) “A superelastic shape-memory-alloy beam,” *Journal of Intelligent Materials and Structures*, vol. 8, pg. 489-501.

Auricchio F., Fugazza D., DesRoches, R. (2006) “Earthquake performance of steel frames with nitinol braces,” *Journal of Earthquake Engineering*, Vol. 10, special issue 1, 45-66.

ACI Committee 318, 2008. *Building code requirements for structural concrete*, (ACI 318-08) and commentary (ACI 318R-08), American Concrete Institute, Formington Hills MI, 444 pp.

Dolce M., Cardone D., Marnetto R., Mucciarelli M., Nigro D., Ponzo F. C., Santarsiero G. (2004) “Experimental Static and dynamic response of a real R/C frame upgraded with SMA re-centring and dissipating braces,” *Proceedings of the 13$^{th}$ World Conference on Earthquake Engineering*, Canada, paper no. 2878.

IBC 2006, International Building Code, International code council, Falls Church, VA.

Mander J.B., Priestley M.J.N. and Park R. (1988) “Theoretical stress-strain model for confined concrete,” *Journal of Structural Engineering*, Vol. 114, No. 8, pp. 1804-1826.

Martinez-Rueda J.E. and Elnashai A.S. (1997) “Confined concrete model under cyclic load,” *Materials and Structures*, Vol. 30, No. 197, pp. 139-147.

Park R. and Paulay T. (1972), *Reinforced Concrete Structures*, John Wiley & Sons, New York.

Paulay T. and Priestley M.J.N. (1992), *Seismic Design of Reinforced Concrete and Masonry Buildings*, John Wiley & Sons, New York.

Sabelli R., Mahin S. and Chang C. (2003) “Seismic demands on steel braced frame buildings with buckling-restrained braces,” *Engineering Structures* 25, 655-666.

SeismoStruct 2009, Version 4.0.2. accessed on Feb 2009, available at http://www.seismosoft.com/SeismoStruct/index.htm.

Vamvatsikos, D. and Cornell, C. A. (2004) “Applied incremental dynamic analysis,” *Earthquake Spectra* 20(2), 523-553.